THE JOURNAL OF PHYSICAL CHEMISTRY LETTERS
A JOURNAL OF THE AMERICAN CHEMICAL SOCIETY

pubs.acs.org/JPCL

Letter

Stretching Bonds without Breaking Symmetries in Density Functional Theory

Yuming Shi, Yi Shi, and Adam Wasserman*

Cite This: *J. Phys. Chem. Lett.* 2024, 15, 826–833

Read Online

ACCESS | Metrics & More | Article Recommendations | Supporting Information

ABSTRACT: Kohn–Sham density functional theory (KS-DFT) stands out among electronic structure methods due to its balance of accuracy and computational efficiency. However, to achieve chemically accurate energies, standard density functional approximations in KS-DFT often need to break underlying symmetries, a long-standing "symmetry dilemma". By employing *fragment* spin densities as the main variables in calculations (rather than total molecular densities, as in KS-DFT), we present an embedding framework in which this symmetry dilemma is understood and partially resolved. The spatial overlap between fragment densities is used as the main ingredient to construct a simple, physically motivated approximation to a universal functional of the fragment densities. This "overlap approximation" is shown to significantly improve semilocal KS-DFT binding energies of molecules without artificially breaking either charge or spin symmetries. The approach is shown to be applicable to covalently bonded molecules and to systems of the "strongly correlated" type.

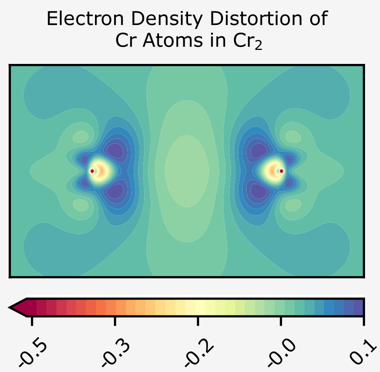

Symmetry breaking occurs in the quantum-mechanical simulation of molecules when the lowest-energy solutions of the electronic Schrödinger equation (SE) do not exhibit the same symmetries of the underlying Hamiltonian. An exact solution of the SE or, equivalently, a solution of the Kohn–Sham equations of Density Functional Theory (KS-DFT)[1,2] with the *exact* exchange–correlation (XC) functional $E_{XC}[n_\uparrow, n_\downarrow]$ yields spin densities $\{n_\uparrow, n_\downarrow\}$ that retain the symmetry of the molecular Hamiltonian. However, it is well-known that spin and charge symmetries of stretched molecules are often broken by density-functional *approximations* (DFAs) for the XC functional. Attempts to prevent such symmetry breaking often lead to qualitatively incorrect electric and magnetic properties of molecules and materials as a consequence of delocalization and static-correlation errors.[3−8] Symmetry breaking, when allowed, can provide insight into the quantum-mechanical correlations that exist between fluctuating charges or spins in the constituent fragments. When these fragments are separated by a large distance $R \to \infty$, the correct (symmetry unbroken) solution of the SE can be understood as an infinite-time average over fluctuations among the possible broken-symmetry solutions.[9]

Consider for example, the spin symmetry of a stretched hydrogen molecule in its singlet ground state. The correct spin-up density $n_\uparrow(\mathbf{r})$ equals the spin-down density $n_\downarrow(\mathbf{r})$ at every point in space, but imposing this symmetry on the solution of the KS-DFT equations with an approximate XC functional (see "RPBE" in panel a of Figure 1 for the popular PBE[10]) leads to unacceptably large energy errors as the molecule is stretched beyond $R \sim 3$ bohr. A broken-symmetry solution exists with an energy that runs close to the exact one ("UPBE" in panel a of Figure 1), with $n_\uparrow(\mathbf{r})$ localized on one atom and $n_\downarrow(\mathbf{r})$ on the other. Although strictly incorrect, this set of spin densities does reflect one of the two possible dissociation channels observed when infinitesimal environmental perturbations induce the collapse of the wave function and breaks the chemical bond.[11]

Similarly, recent studies show that the SCAN meta-GGA funcional[12] can yield highly accurate binding energies for a great number of systems including some of the "strongly correlated" type,[13−17] but only when spin-symmetry breaking is allowed. A question then arises on the interpretation of such broken-symmetry solutions for *finite* *R*.[18] These are useful, among others, to calculate values of magnetic properties of molecules such as exchange-coupling constants.[19,20]

Is it possible to calculate accurate energies *without* breaking symmetries when employing standard (e.g., PBE, SCAN) XC functionals? In this work we join others who have provided a positive answer,[21−27] but from an entirely different perspective. We introduce a partitioning-based approach to address the challenge, marking a systematic improvement on the model initially proven successful in singly bonded systems.[28] Our method clarifies the underlying challenge by rectifying violations of exact conditions of nonadditive functionals from

Received: November 1, 2023
Revised: December 22, 2023
Accepted: December 28, 2023
Published: January 17, 2024

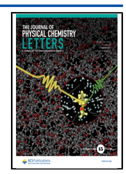

https://doi.org/10.1021/acs.jpclett.3c03073
J. Phys. Chem. Lett. 2024, 15, 826–833

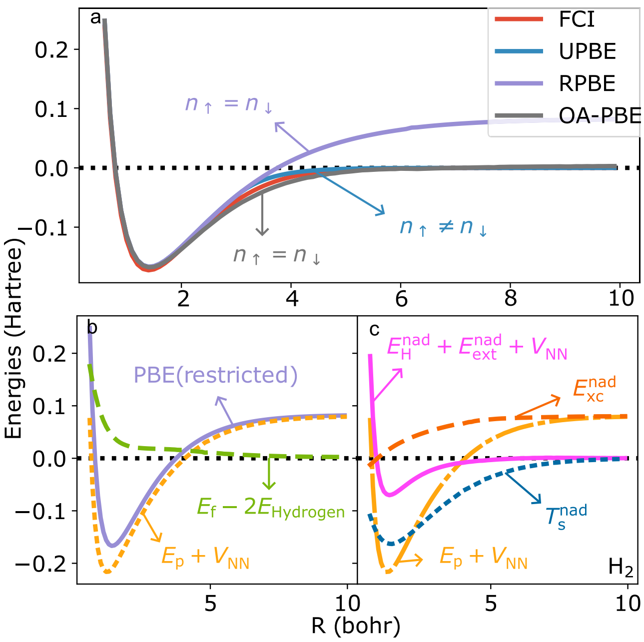

Figure 1. (a) Binding energy of H_2 calculated through (i) FCI reference values (red), (ii) spin-unrestricted PBE (UPBE blue), (iii) spin-restricted PBE (RPBE purple), and (iv) OA-PBE from eqs 4 and 5 (gray). (b) restricted-PBE energies (purple) decomposed: Fragment relaxation energies are $E_f - 2E_{\text{Hydrogen}}$ (green) and partition energy $E_p + V_{NN}$ (yellow). V_{NN} is nuclear−nuclear repulsion. (c) Decomposition of E_p (yellow) into nonadditive kinetic (blue), exchange−correlation (orange), and all remaining contributions (pink). Note that the large error of the restricted-PBE calculation as $R \to \infty$ can be attributed almost entirely to E_{XC}^{nad}.

KS-DFT, and showcases its success through the enforcement of these conditions in more complex systems. The key is to use a formulation of DFT in which (1) electronic *fragment* spin densities (as an alternative to total molecular densities) are sharply defined for finite R and recover those of isolated atoms as $R \to \infty$, (2) each of those fragment spin densities is described through a mixed-state ensemble that can place fractional charges and spins on the fragments to guarantee the correct symmetries, and (3) there exists a universal functional of the set of fragment spin densities that describes the fragment interaction and is amenable to simple yet accurate approximations.

All three of these features are provided by Partition-DFT (P-DFT),[29,30] a formally exact density embedding method in which a molecule, defined by a nuclear "external" potential $v(\mathbf{r}) = \sum_\alpha^{N_{\text{frag}}} v_\alpha(\mathbf{r})$ and N electrons, is partitioned into N_{frag} smaller fragments (labeled by α). The features listed above are met in the following way: (1) The fragment spin densities are uniquely defined by the requirement that the sum of fragment energies E_f be minimized under the constraint that the sum of fragment spin densities $n_{f,\sigma}(\mathbf{r}) \equiv \sum_\alpha^{N_{\text{frag}}} n_{\alpha,\sigma}(\mathbf{r})$ matches the correct spin density $n_\sigma(\mathbf{r})$ of the molecule, i.e., the ground-state spin density for N electrons in $v(\mathbf{r})$. The Lagrange multiplier that enforces this constraint is a unique *partition potential* $v_p(\mathbf{r})$.[31] (2) Each of the fragment spin densities $n_{\alpha,\sigma}(\mathbf{r})$ is a ground-state *ensemble* density for a (possibly fractional) number of electrons and spins in $v_\alpha(\mathbf{r}) + v_p(\mathbf{r})$. (3) A universal functional $Q[\mathbf{n}]$ of the set of fragment spin densities $\mathbf{n} \equiv \{n_{\alpha,\sigma}\}$ is defined as

$$Q[\mathbf{n}] = F[n_\uparrow, n_\downarrow] - \sum_\alpha^{N_{\text{frag}}} \min_{\hat{\rho}_\alpha \to \{n_{\alpha,\uparrow}, n_{\alpha,\downarrow}\}} \text{Tr}(\hat{\rho}_\alpha(\hat{T} + \hat{V}_{ee})) \quad (1)$$

with

$$F[n_\uparrow, n_\downarrow] = \min_{\Psi \to \{n_\uparrow, n_\downarrow\}} \langle \Psi | \hat{T} + \hat{V}_{ee} | \Psi \rangle \quad (2)$$

as the spin-decomposed[32] Levy−Lieb functional;[33,34] $\hat{T}$ and $\hat{V}_{ee}$ are the kinetic and electron−electron repulsion operators. The search inside the sum in eq 1 is performed over fragment density matrices $\hat{\rho}_\alpha$ yielding the preset pairs of fragment spin densities $\{n_{\alpha,\uparrow}, n_{\alpha,\downarrow}\}$ and the search in eq 2 is performed over normalized, antisymmetric electronic N-electron wave functions Ψ yielding the total spin densities $n_\uparrow$ and $n_\downarrow$. When evaluated at the unique set $\mathbf{n}$ of fragment spin densities minimizing E_f, the ground-state energy of the molecule is then given by

$$E = E_f[\mathbf{n}] + E_p[\mathbf{n}] \quad (3)$$

where E_f is the fragment energy summation without the contribution from the partition potential ($E_f = \sum_\alpha^{N_{\text{frag}}} E_\alpha$) and the *partition energy* E_p has been defined as the rest $E_p[\mathbf{n}] = Q[\mathbf{n}] + \int d\mathbf{r}\, v(\mathbf{r})\, n_f(\mathbf{r}) - \sum_{\alpha,\sigma}^{N_{\text{frag}}} \int d\mathbf{r}\, v_\alpha(\mathbf{r})\, n_{\alpha,\sigma}(\mathbf{r})$. It can be proven[30] that the partition potential $v_p(\mathbf{r})$ is the functional derivative of E_p evaluated for a given set of fragment spin-densities $\mathbf{n}$.

It is useful to decompose $Q[\mathbf{n}]$ in terms of the usual Kohn−Sham density functional quantities as the sum of three *nonadditive* (nad) terms: $Q[\mathbf{n}] = T_s^{\text{nad}}[\mathbf{n}] + E_H^{\text{nad}}[\mathbf{n}] + E_{XC}^{\text{nad}}[\mathbf{n}]$, where, e.g., $E_{XC}^{\text{nad}}[\mathbf{n}] = E_{XC}[n_f] - \sum_\alpha^{N_{\text{frag}}} E_{XC}[n_\alpha]$. One can then see that most of the PBE error for stretched H_2, for example, is contained in E_p (panel b of Figure 1) and, more specifically, in E_{XC}^{nad} (panel c). Various strategies for approximating the KS kinetic term, $T_s^{\text{nad}}[\mathbf{n}]$, are being investigated[35−37] but here we compute this term *exactly* via density-to-potential inversions.[38−41] Thus, for a given approximation to $E_{XC}[n]$, the P-DFT calculations simply reproduce the results of KS-DFT, including all of their errors (purple lines in Figure 1). Here we argue that almost all of the error of PBE at dissociation can be attributed to the unphysical behavior of $E_{XC}^{\text{nad}}(R)$ and can be suppressed through improved approximations for this term alone. The gray line labeled OA-PBE in panel a of Figure 1, for example, shows how a simple "overlap approximation" for $E_{XC}^{\text{nad}}[\mathbf{n}]$ (to be defined below) removes most of the PBE error while preserving the correct spin symmetry as $R \to \infty$.

We demonstrate that accurate binding energies for stretched molecules can be obtained through physically motivated approximations for $E_{XC}^{\text{nad}}[\mathbf{n}]$ *without* symmetry breaking. We begin with the simplest case of closed-shell molecules partitioned into $N_{\text{frag}} = 2$ fragments with spin-summed fragment densities $n_A(\mathbf{r})$ and $n_B(\mathbf{r})$ using a standard GGA funcional (PBE). For all such cases, like in H_2, $E_{XC,\text{PBE}}^{\text{nad}}(R)$ goes to an incorrect positive constant as $R \to \infty$ rather than satisfying the *exact constraint*: $E_{XC}^{\text{nad}}[\mathbf{n}](R) \to 0$. We now build this constraint into $E_{XC}^{\text{nad}}[\mathbf{n}]$ through a simple model:

$$E_{XC,\text{PBE}}^{\text{nad,OA}}[\mathbf{n}] = S[\mathbf{n}] E_{XC,\text{PBE}}^{\text{nad}} \quad (4)$$

$$S[\mathbf{n}] = \text{erf}\left[\frac{C}{D[\mathbf{n}]} \int d\mathbf{r}\, (n_A(\mathbf{r})\, n_B(\mathbf{r}))^p\right] \quad (5)$$

The overlap integral $\int d\mathbf{r}\, (n_A(\mathbf{r})\, n_B(\mathbf{r}))^p$ in the error function is found to capture a wide range of bond forming/breaking

https://doi.org/10.1021/acs.jpclett.3c03073
J. Phys. Chem. Lett. 2024, 15, 826−833

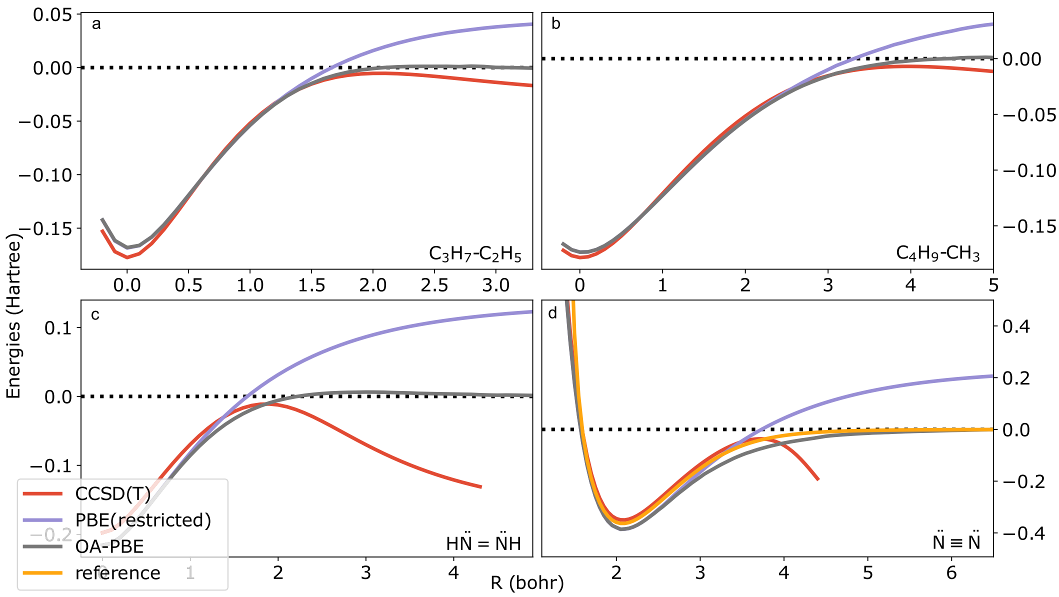

Figure 2. Using PBE for the fragments, eqs 4 and 5 with $C = 2$ and $p = 1/2$ yield accurate binding energies (gray) when cutting through single ($D = 1$), double ($D = 2$), and triple ($D = 3$) bonds. Comparisons are made with spin-restricted PBE (purple), CCSD(T) (red), or reference values from ref 42 (yellow). In panels a and b, 0 on the x-axis is defined as equilibrium.

scenarios. The prefactor $\frac{C}{D[\mathbf{n}]}$ ensures that the density overlap is scaled correctly to the domain of the error function. $D[\mathbf{n}]$ is itself a functional of the set of fragment densities, offering the flexibility needed for eq 4 to satisfy known exact conditions.[43] In this work, we approximate $D[\mathbf{n}]$ not as an *explicit* functional of $\mathbf{n}$, but as a number that depends on the nature of the chemical bond being stretched. When fixing $C = 2$, we find that $D[\mathbf{n}]$ takes on especially suggestive values for *single* (A−B), *double* (A═B), or *triple* (A≡B) bonds:

$$D[\mathbf{n}] \cong \begin{cases} 1, & A-B \\ 2, & A=B \\ 3, & A\equiv B \end{cases} \tag{6}$$

Generally, p is also a functional of fragment densities $p = p[\mathbf{n}]$. Under the constant-D approximation of eq 6, p is set to 1/2 to ensure that $S[\mathbf{n}]$ is dimensionless. The constant-D approximation is not fitted to particular systems but rather approximates the valence electron densities. This simple approximation preserves the description of PBE around equilibrium while correcting the PBE errors as these build up beyond the Coulson−Fisher point (see curve labeled "OA-PBE" in Figure 1). Equations 4−6 perform extremely well for singly bonded hydrocarbons, as well as doubly bonded diazene, and triply bonded nitrogen molecules, systems that are famously challenging for standard DFAs,[4] and also for the "gold standard" of quantum chemistry methods, CCSD(T) (coupled-cluster with single and double and perturbative triple excitations);[44] see Figure 2. It should be noted in Figure 2 that the energies sometimes approach the right dissociation limit from the wrong direction (above). This is partly due to the constant D approximation in eq 6 which overestimates the bond strength as fragments are stretched apart.

The approximation defined by eq 6 is inadequate for molecules that are even more "strongly correlated" than N_2. Consider the challenging case of the chromium dimer (Cr_2). A quantitative description of the electronic structure of Cr_2 is a stringent test for any theory that attempts to capture strong correlations in molecules. Neither CASSCF nor CCSD(T) yield quantitative agreement for the ground-state energy of Cr_2 as a function of the internuclear separation. As is well-known, standard DFAs in KS-DFT are utterly inadequate to capture the multireference character of the ground state in stretched Cr_2.[46,47] Only very recently has a truly *ab initio* calculation been reported for Cr_2.[45] Unsurprisingly, Figure 3 shows that the OA-PBE of eqs 4 and 5 for convalent bonds with $D = 6$ ($C = 2$ fixed, see "OA-PBE" in panel b) does improve but not

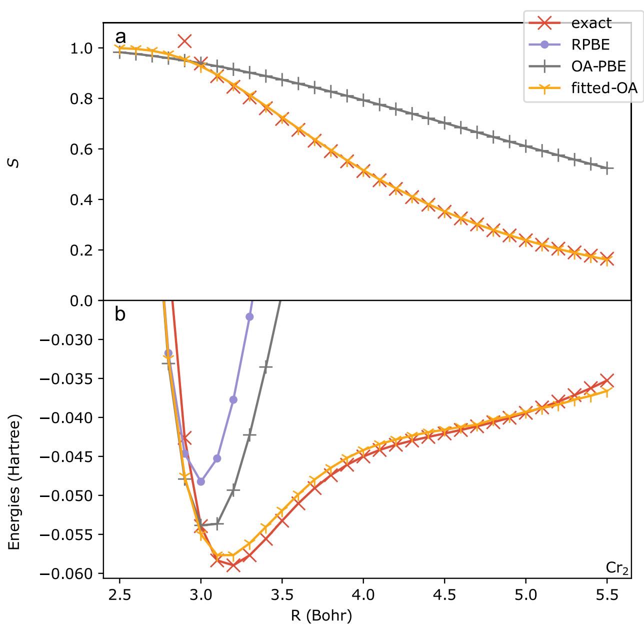

Figure 3. (a) $S(R)$ for Cr_2 obtained from (i) numerically exact results from ref 45 (red, exact), (ii) eq 5 with $p = 1/2$, and $D = 6$ (gray, OA-PBE), and (iii) fitted with $D = 1.15$, $p = 0.8$ (yellow, fitted-OA-PBE). (b) Corresponding binding energies, where pure restricted-PBE has been included for comparison (purple).

https://doi.org/10.1021/acs.jpclett.3c03073
J. Phys. Chem. Lett. 2024, 15, 826−833

enough to match the *ab initio* results, as the interfragment interaction in Cr_2 is radically different than in the molecules of Figure 2.

In order to further investigate our assumption that most XC DFA errors originate from the E_{XC}^{nad}, we calculate the *exact* $S_{exact}[\mathbf{n}] = E_{XC,\ exact}^{nad}[\mathbf{n}]/E_{XC,\ DFA}^{nad}[\mathbf{n}]$, where $E_{XC,\ DFA}^{nad}[\mathbf{n}]$ is the nonadditive exchange correlation energy obtained through a self-consistent P-DFT calculation that uses a DFA for the XC energy functional. With access to accurate total energies,[45] one can extract $E_{XC,exact}^{nad}[\mathbf{n}]$ by subtraction of the other components available exactly from P-DFT calculations. The behavior of $S_{exact}(R)$ can then be examined as illustrated in panel a of Figure 3. A fitted model "fitted-OA" in Figure 3, using $p = 0.8$ in the integrand of eq 5 and the value $D = 1.15$ in the denominator leads to quantitative agreement between the OA energies and the most accurate (but expensive) state-of-the-art *ab initio* calculations for all internuclear separations (see yellow lines in Figure 3). This fitted approximation for Cr_2 is oversimplified by fixing $D[\mathbf{n}]$ and p for a more complex functional. Thus, it only agrees with the exact results for a range of separations (as one can see, the disagreement starts appearing at R = 5.5 Bohr), but it illustrates the potential of the OA approach for systems that exhibit abnormally high electron correlation effects. The simplicity of eqs 4−6 and smoothness of $S_{exact}(R)$ (see panel a of Figure 3), especially in regions where $E(R)$ varies quite rapidly with R (see panel b of Figure 3) illustrate the usefulness of correcting E_{XC}^{nad}.

The obvious question is how the overlap functional should be further improved to be more generally applicable and predictive. So far, we have shown how our understanding of the symmetry dilemma, as illustrated in Figure 1, can lead to a physically sound approximation to the partition energy. The general form of the overlap approximation (eqs 4 and 5) together with further approximations for $D[\mathbf{n}]$ correct for different types of bond breaking that regular XC DFAs are unable to describe for different types of interactions. However, even in the systems presented in this Letter there are regions in the binding curves where the corrections are overestimated. These together suggest that it should be possible and worthwhile to derive a more general functional for $S[\mathbf{n}]$ from first-principles and more exact conditions.

Before moving on to considering the case of charge symmetry, we provide a proof-of-principle demonstration that the same idea (eqs 4 and 5) can be extended to an arbitrary number of fragments $N_{frag} > 2$. When there are more fragments and P-DFT yields a set of densities $\mathbf{n} = \{n_1(\mathbf{r}), n_2(\mathbf{r}), ..., n_{N_{frag}}(\mathbf{r})\}$, it is important to consider the pairwise interactions between the fragments. To achieve this, we developed a nested version of the OA (NOA) where eq 4 can be applied recursively:

$$E_{XC}^{nad,NOA}[\mathbf{n}] = S[\mathbf{n}_{1\to m}, \mathbf{n}_{m+1\to N_{frag}}]\, E_{XC}^{nad}[\mathbf{n}_{1\to m}, \mathbf{n}_{m+1\to N_{frag}}] + E_{XC}^{nad,NOA}[\mathbf{n}_{1\to m}] + E_{XC}^{nad,NOA}[\mathbf{n}_{m+1\to N_{frag}}] \quad (7)$$

where $\mathbf{n}_{a\to d}$ denotes the partial sum of fragment densities $n_a(\mathbf{r}) + ... + n_d(\mathbf{r})$. In eq 7, $D[\mathbf{n}_{1\to m}, \mathbf{n}_{m+1\to N_{frag}}]$ at each level could be different, depending on the fragment densities of the two branches. As for the case of binary fragmentation, this prescription preserves the results of the parent DFA at equilibrium separations and can improve the results when bonds are stretched. We have tested eq 7 on hydrogen chains with the overlap model of eq 5, which is a case of multiple bonds (single bonds $D[\mathbf{n}] = 1$) breaking simultaneously and the results demonstrate that eq 7 corrects the errors of PBE as $R \to \infty$ (see Figure 4 for H_{10}, a well-known test-bed for strongly correlated systems[48]), although it underestimates the corrections needed in the intermediate range $2.5 < R < 4$ bohr. More research into the form of eq 7 and its accompanying overlap measure is clearly needed.

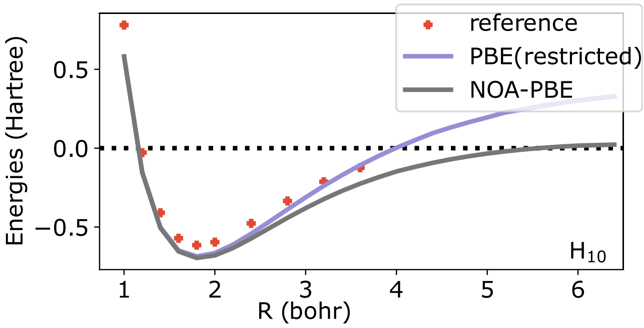

Figure 4. NOA of eq 7 corrects the PBE error for the binding energies in hydrogen chains as $R \to \infty$ (here H_{10}, where the *x*-axis is the distance R between neighboring nuclei). The reference is the Multireference Configuration Interaction taken from ref 48.

We now discuss *charge symmetry*, which is analogous to the case of spin symmetry but with an extra challenge. First, the analogy: As in the case of spin symmetry that we have just discussed, the approximation chosen for $E_{XC}[n_\uparrow, n_\downarrow]$ will typically lead to improved energies when charge symmetries are broken. The extra challenge: The charge-symmetry-broken solutions are typically *higher* in energy than the charge-symmetric solutions and will therefore not be found when searching for a minimum. In other words: The analogue of spin-unrestricted calculations will not lead to improved energies. Take, for example, the case of stretched H_2^+ in Figure 5, where PBE underestimates the dissociation energy by 70%. The PBE ground-state energy of an isolated hydrogen atom is only off by 0.08%, so the dissociation energy error can be attributed almost entirely in this case to the fact that the KS equations *not* break the charge symmetry of the ground state. How can one keep that symmetry *and* correct the energy? Again, as before, we analyze the contributions to $Q[\mathbf{n}]$ from the different KS components and find that, this time, the problem is not fixed by simply quenching $E_{XC}^{nad}(R)$ for large R because, for any given R, $E_{XC}^{nad}(R)$ does not cancel $E_H^{nad}(R)$ as it should for a 1-electron system (see panel c of Figure 5). This *nonadditive self-interaction error* can be corrected approximately by adding a term to E_{XC}^{nad} in eq 4:

$$E_{XC}^{nad,OA}[\mathbf{n}] = S[\mathbf{n}]E_{XC,PBE}^{nad} + (1 - S[\mathbf{n}])\Delta E_{\mathbf{H}}^{nad} \quad (8)$$

$$\Delta E_H^{nad} = \sum_{i,j}^{\text{ensemble}} g_{ij} \int \frac{n_{A,i}(\mathbf{r})\, n_{B,j}(\mathbf{r}')}{|\mathbf{r} - \mathbf{r}'|}\, d\mathbf{r}\, d\mathbf{r}' - E_H^{nad} \quad (9)$$

where $g_{ij} = 1$ when $N_{Ai,\sigma} + N_{Bj,\sigma} = N_\sigma$ and $g_{ij} = 0$ otherwise, implying the possible dissociation channels.

With this choice of g_{ij}, eq 8 reduces to eq 4 for closed-shell systems but improves over eq 4 for open shells, as shown by the gray line labeled "OA-PBE" in Figure 5 for H_2^+ with $D[\mathbf{n}] = 1$ and in ref 28 for Li_2^+.

https://doi.org/10.1021/acs.jpclett.3c03073
J. Phys. Chem. Lett. 2024, 15, 826−833

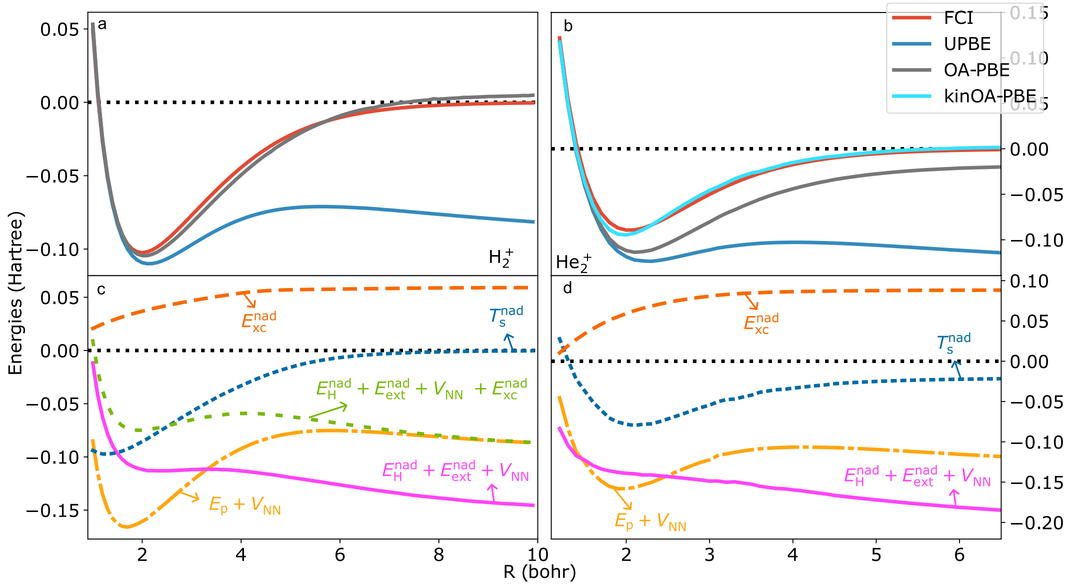

Figure 5. (a) H_2^+ binding energies were calculated with FCI (red), PBE (blue), and OA-PBE (gray). (b) He_2^+ binding energies, including a kinOA calculation in which $Q = ST_s^{nad} + E_H^{nad} + E_{XC,PBE}^{nad,OA}[\mathbf{n}]$ (light blue). (c,d) Components of E_p showing that the PBE error can be attributed to a poor cancellation of errors between E_{XC}^{nad} and E_H^{nad}.

Equations 8 and 9, together with the model for $S[\mathbf{n}]$ of eqs 5 and 6 can even significantly improve the PBE binding energies of He_2^+, a challenging molecule for reasons other than delocalization and static correlation.[49] The agreement between OA-PBE and FCI in this case is not quantitative (panel b in Figure 5), but P-DFT calculations indicate that the remaining source of error belongs to $T_s^{nad}(R)$, probably due to the difficulties associated with finding a pure-state spin density for such a stretched system,[50−52] leading to a nonzero $T_s^{nad}(R)$ as $R \to \infty$ (see panel d of Figure 5). However, the results labeled by "kinOA-PBE" in panel b of Figure 5 demonstrate that this error can be suppressed almost entirely by multiplying T_s^{nad} by $S[\mathbf{n}]$ and approximating $Q[\mathbf{n}]$ as $Q[\mathbf{n}] \approx S[\mathbf{n}]T_s^{nad}[\mathbf{n}] + E_{HXC,PBE}^{nad,OA}[\mathbf{n}]$. This is not as physically meaningful as for eq 4 and eq 8 but again proves the accuracy of the approximations we made in eqs 5 and 6 describing covalent bond breaking.

By using molecular spin densities $\{n_\uparrow(\mathbf{r}), n_\downarrow(\mathbf{r})\}$ as the main variables in calculations, XC approximations are hard-pressed to describe the low-density internuclear regions of molecules where correlation effects are relatively more important (compared to kinetic effects), so the XC approximations are in a sense blind to the formation of fragments when bonds are stretched. Methods including symmetry-breaking,[18,19] self-interaction error corrections,[32,53−56] range-separated functionals,[57−62] double hybrid functionals,[63,64] and scaling correction methods[65] are all among approaches that have been adopted to overcome such difficulties. Moreover, methods relying on manual exact-condition enforcement through neural-network training,[21] the "on-top" pair density,[22,23,66] complex orbitals,[24] exact strong-interaction limit functionals,[25] and fractional-spin localized orbital scaling corrections[26,67] can improve the accuracy for systems of the strongly correlated type. Recognizing that such strongly correlated systems are often composed of weakly overlapping fragments,[68,69] the central result of our work is that, when *fragment* spin densities are used as the main variables, the typical delocalization and static-correlation errors of approximate $E_{XC}[n_\uparrow, n_\downarrow]$[3−8] can be largely avoided without having to abandon essential symmetries. This alternative strategy rests on maintaining the use of the same approximate $E_{XC}[\{n_{\alpha,\uparrow}, n_{\alpha,\downarrow}\}]$ *within* the fragments while introducing new interfragment approximations for $E_{XC}^{nad}[\mathbf{n}]$. The latter is a functional of the set of fragment spin densities $\mathbf{n}$ rigorously defined within P-DFT.[30]

Two exact constraints satisfied by $E_{XC}^{nad}[\mathbf{n}]$ were used in the construction of eq 8: (1) $E_{XC}^{nad}[\mathbf{n}] \to 0$ as $R \to \infty$, where R denotes the separation between fragments and (2) $E_{XC}^{nad}[\mathbf{n}] \to -E_H^{nad}[\mathbf{n}]$ for single-electron bonds. Equation 8, and the accompanying model for $S[\mathbf{n}]$ in eqs 5 and 6, should be seen as initial attempts at approximating these quantities. Future approximations of $E_{XC}^{nad}[\mathbf{n}]$ should incorporate more exact constraints. For example, how could eqs 4 and 5 be improved to encompass van der Waals interactions?[70,71] How could the $D[\mathbf{n}]$ functional be improved beyond eq 6 to properly scale the overlap integral while preserving the exact conditions obeyed by the underlying XC functional?[43]

■ METHODS

All calculations were done using a P-DFT implementation in *Psi4*.[72] The cc-pVTZ basis set was used for all molecules in this work except for the cases of H_{10} and Cr_2, for which cc-pVDZ and cc-pV5Z were used instead. P-DFT PBE calculations (without the OA) converge to the same results as the direct restricted-PBE KS-DFT (with the KS-inversion). The Wu−Yang algorithm[38] implemented on Gaussian basis sets in *n2v*[40] was used to calculate all $T_s[n_f]$ components. The OA was performed as a post-PDFT approximation, i.e., using the fragment densities yielded by P-DFT.[28] The details for the numerical implementation as well as convergence can be found in the Supporting Information. Functional-driven error domination is assumed. Convergence of the partition potential v_p was achieved in each case by updating it iteratively according to

$$v_p^{k+1} = v_p^k + \lambda(v_{XC,PBE}[n_f] - v_{XC,inv}[n_f]) \tag{10}$$

https://doi.org/10.1021/acs.jpclett.3c03073
J. Phys. Chem. Lett. 2024, 15, 826−833

for the $(k+1)^{\text{th}}$ step, where λ is the step size. $v_{\text{XC,PBE}}[n_f]$ is the XC potential for a choice of XC approximation (we use PBE in this article). $v_{\text{xc,inv}}$ is the effective partition potential calculated from inversion, as explained by eq 13 below. The derivation of eq 10 is outlined next, omitting spin indices for simplicity. Start from the definition of v_p[30] as $v_p = \frac{\delta E_p}{\delta n_\alpha}$, where n_α is the density for fragment α. At convergence, the same v_p is shared by all fragments and is independent of the fragment index α. By separating E_p as suggested in the main text, v_p is decomposed as

$$v_p(\mathbf{r}) = \frac{\delta T_s[n_f]}{\delta n_f(\mathbf{r})} - \frac{\delta T_s[n_\alpha]}{\delta n_\alpha(\mathbf{r})} + v(\mathbf{r}) - v_\alpha(\mathbf{r}) + v_H[n_f](\mathbf{r}) - v_H[n_\alpha](\mathbf{r}) + v_{\text{XC,PBE}}[n_f](\mathbf{r}) - v_{\text{XC,PBE}}[n_\alpha](\mathbf{r}) \tag{11}$$

Given that stationary condition for the fragments at each step k

$$\frac{\delta T_s[n_\alpha]}{\delta n_\alpha(\mathbf{r})} + v_\alpha(\mathbf{r}) + v_H[n_\alpha](\mathbf{r}) + v_{\text{XC,PBE}}[n_\alpha](\mathbf{r}) + v_p = \mu_\alpha \tag{12}$$

as well as for the entire system through inversion

$$\frac{\delta T_s[n_f]}{\delta n_f(\mathbf{r})} + v(\mathbf{r}) + v_H[n_f](\mathbf{r}) + v_{\text{XC,inv}}[n_f](\mathbf{r}) = \mu \tag{13}$$

Equation 10 follows by omitting the chemical potentials since μ provides no energy contribution to the total energy.

ASSOCIATED CONTENT

Supporting Information

The Supporting Information is available free of charge at https://pubs.acs.org/doi/10.1021/acs.jpclett.3c03073.

Electron configuration and ensemble treatment for fragments with fractional numbers of electrons and partition density functional theory computational details (PDF)

Transparent Peer Review report available (PDF)

AUTHOR INFORMATION

Corresponding Author

Adam Wasserman − *Department of Physics and Astronomy and Department of Chemistry, Purdue University, West Lafayette, Indiana 47907, United States;* orcid.org/0000-0002-8037-4453; Email: awasser@purdue.edu

Authors

Yuming Shi − *Department of Physics and Astronomy, Purdue University, West Lafayette, Indiana 47907, United States;* orcid.org/0009-0001-0552-1003

Yi Shi − *Department of Chemistry, Purdue University, West Lafayette, Indiana 47907, United States;* orcid.org/0009-0009-7918-5821

Complete contact information is available at: https://pubs.acs.org/10.1021/acs.jpclett.3c03073

Notes

The authors declare no competing financial interest.

ACKNOWLEDGMENTS

Discussions with Kieron Burke are gratefully acknowledged. This work was supported by the U.S. National Science Foundation under Grant No. CHE-2306011. Calculations used *Anvil* at *Purdue* through allocation OTH220004 from the Advanced Cyberinfrastructure Coordination Ecosystem: Services & Support (ACCESS) program.[73] Acknowledgement is also made to the donors of the American Chemical Society Petroleum Research Fund for partial support of this research under grant No. 62544-ND6.

REFERENCES

(1) Hohenberg, P.; Kohn, W. Inhomogeneous electron gas. *Phys. Rev.* **1964**, *136*, B864.

(2) Kohn, W.; Sham, L. J. Self-consistent equations including exchange and correlation effects. *Phys. Rev.* **1965**, *140*, A1133.

(3) Burke, K. Perspective on density functional theory. *J. Chem. Phys.* **2012**, *136*, 150901.

(4) Cohen, A. J.; Mori-Sánchez, P.; Yang, W. Challenges for density functional theory. *Chem. Rev.* **2012**, *112*, 289−320.

(5) Mardirossian, N.; Head-Gordon, M. Thirty years of density functional theory in computational chemistry: an overview and extensive assessment of 200 density functionals. *Mol. Phys.* **2017**, *115*, 2315−2372.

(6) Becke, A. D. Perspective: Fifty years of density-functional theory in chemical physics. *J. Chem. Phys.* **2014**, *140*, 18A301.

(7) Perdew, J. P.; Parr, R. G.; Levy, M.; Balduz, J. L., Jr Density-functional theory for fractional particle number: derivative discontinuities of the energy. *Phys. Rev. Lett.* **1982**, *49*, 1691.

(8) Mori-Sánchez, P.; Cohen, A. J.; Yang, W. Discontinuous nature of the exchange-correlation functional in strongly correlated systems. *Phys. Rev. Lett.* **2009**, *102*, No. 066403.

(9) Anderson, P. W. An approximate quantum theory of the antiferromagnetic ground state. *Phys. Rev.* **1952**, *86*, 694.

(10) Perdew, J. P.; Burke, K.; Ernzerhof, M. Generalized gradient approximation made simple. *Phys. Rev. Lett.* **1996**, *77*, 3865.

(11) Levine, D. S.; Head-Gordon, M. Clarifying the quantum mechanical origin of the covalent chemical bond. *Nat. Commun.* **2020**, *11*, 4893.

(12) Sun, J.; Ruzsinszky, A.; Perdew, J. P. Strongly constrained and appropriately normed semilocal density functional. *Phys. Rev. Lett.* **2015**, *115*, No. 036402.

(13) Furness, J. W.; Zhang, Y.; Lane, C.; Buda, I. G.; Barbiellini, B.; Markiewicz, R. S.; Bansil, A.; Sun, J. An accurate first-principles treatment of doping-dependent electronic structure of high-temperature cuprate superconductors. *Commun. Phys.* **2018**, *1*, 11.

(14) Zhang, Y.; Lane, C.; Furness, J. W.; Barbiellini, B.; Perdew, J. P.; Markiewicz, R. S.; Bansil, A.; Sun, J. Competing stripe and magnetic phases in the cuprates from first principles. *Proc. Natl. Acad. Sci. U.S.A.* **2020**, *117*, 68−72.

(15) Kitchaev, D. A.; Peng, H.; Liu, Y.; Sun, J.; Perdew, J. P.; Ceder, G. Energetics of MnO 2 polymorphs in density functional theory. *Phys. Rev. B* **2016**, 93, No. 045132.

(16) Liu, J.; Yu, J.; Ning, J. L.; Yi, H.; Miao, L.; Min, L.; Zhao, Y.; Ning, W.; Lopez, K.; Zhu, Y.; et al. Spin-valley locking and bulk quantum Hall effect in a noncentrosymmetric Dirac semimetal BaMnSb2. *Nat. Commun.* **2021**, *12*, 4062.

(17) Perdew, J. P.; Chowdhury, S. T. u. R.; Shahi, C.; Kaplan, A. D.; Song, D.; Bylaska, E. J. Symmetry breaking with the SCAN density functional describes strong correlation in the singlet carbon dimer. *J. Phys. Chem. A* **2023**, *127*, 384−389.

(18) Perdew, J. P.; Ruzsinszky, A.; Sun, J.; Nepal, N. K.; Kaplan, A. D. Interpretations of ground-state symmetry breaking and strong correlation in wavefunction and density functional theories. *Proc. Natl. Acad. Sci. U.S.A.* **2021**, *118*, e2017850118.

(19) Noodleman, L. Valence bond description of antiferromagnetic coupling in transition metal dimers. *J. Chem. Phys.* **1981**, *74*, 5737−5743.

(20) Dai, D.; Whangbo, M.-H. Spin-Hamiltonian and density functional theory descriptions of spin exchange interactions. *J. Chem. Phys.* **2001**, *114*, 2887−2893.

(21) Kirkpatrick, J.; McMorrow, B.; Turban, D. H.; Gaunt, A. L.; Spencer, J. S.; Matthews, A. G.; Obika, A.; Thiry, L.; Fortunato, M.; Pfau, D.; et al. Pushing the frontiers of density functionals by solving the fractional electron problem. *Science* **2021**, *374*, 1385−1389.
(22) Perdew, J. P.; Savin, A.; Burke, K. Escaping the symmetry dilemma through a pair-density interpretation of spin-density functional theory. *Phys. Rev. A* **1995**, *51*, 4531.
(23) Li Manni, G.; Carlson, R. K.; Luo, S.; Ma, D.; Olsen, J.; Truhlar, D. G.; Gagliardi, L. Multiconfiguration pair-density functional theory. *J. Chem. Theory Comput.* **2014**, *10*, 3669−3680.
(24) Lee, J.; Bertels, L. W.; Small, D. W.; Head-Gordon, M. Kohn-sham density functional theory with complex, spin-restricted orbitals: Accessing a new class of densities without the symmetry dilemma. *Phys. Rev. Lett.* **2019**, *123*, 113001.
(25) Malet, F.; Gori-Giorgi, P. Strong correlation in Kohn-Sham density functional theory. *Phys. Rev. Lett.* **2012**, *109*, 246402.
(26) Su, N. Q.; Li, C.; Yang, W. Describing strong correlation with fractional-spin correction in density functional theory. *Proc. Natl. Acad. Sci. U.S.A.* **2018**, *115*, 9678−9683.
(27) Gu, Y.; Xu, X. Symmetry Dilemma of Doubly Hybrid Density Functionals for Equilibrium Molecular Property Calculations. *J. Chem. Theory Comput.* **2021**, *17*, 7745−7752.
(28) Nafziger, J.; Wasserman, A. Fragment-based treatment of delocalization and static correlation errors in density-functional theory. *J. Chem. Phys.* **2015**, *143*, 234105.
(29) Elliott, P.; Burke, K.; Cohen, M. H.; Wasserman, A. Partition density-functional theory. *Phys. Rev. A* **2010**, *82*, No. 024501.
(30) Nafziger, J.; Wasserman, A. Density-based partitioning methods for ground-state molecular calculations. *J. Phys. Chem. A* **2014**, *118*, 7623−7639.
(31) Cohen, M. H.; Wasserman, A. On hardness and electronegativity equalization in chemical reactivity theory. *J. Stat. Phys.* **2006**, *125*, 1121−1139.
(32) Perdew, J. P.; Zunger, A. Self-interaction correction to density-functional approximations for many-electron systems. *Phys. Rev. B* **1981**, *23*, 5048.
(33) Levy, M. Universal variational functionals of electron densities, first-order density matrices, and natural spin-orbitals and solution of the v-representability problem. *Proc. Natl. Acad. Sci. U.S.A.* **1979**, *76*, 6062−6065.
(34) Lieb, E. H. Density functionals for Coulomb systems. *Int. J. Quantum Chem.* **1983**, *24*, 243−277.
(35) Shao, X.; Mi, W.; Pavanello, M. GGA-level subsystem DFT achieves Sub-kcal/mol accuracy intermolecular interactions by mimicking nonlocal functionals. *J. Chem. Theory Comput.* **2021**, *17*, 3455−3461.
(36) Jiang, K.; Nafziger, J.; Wasserman, A. Non-additive non-interacting kinetic energy of rare gas dimers. *J. Chem. Phys.* **2018**, *148*, 104113.
(37) Polak, E.; Englert, T.; Gander, M. J.; Wesolowski, T. A. Symmetrized non-decomposable approximations of the non-additive kinetic energy functional. *J. Chem. Phys.* **2023**, *158*, 174107.
(38) Wu, Q.; Yang, W. A direct optimization method for calculating density functionals and exchange−correlation potentials from electron densities. *J. Chem. Phys.* **2003**, *118*, 2498−2509.
(39) Shi, Y.; Wasserman, A. Inverse Kohn−Sham density functional theory: progress and challenges. *J. Phys. Chem. Lett.* **2021**, *12*, 5308−5318.
(40) Shi, Y.; Chávez, V. H.; Wasserman, A. n2v: A density-to-potential inversion suite. A sandbox for creating, testing, and benchmarking density functional theory inversion methods. *Wiley Interdiscip. Rev. Comput. Mol. Sci.* **2022**, *12*, e1617.
(41) Kanungo, B.; Zimmerman, P. M.; Gavini, V. Exact exchange-correlation potentials from ground-state electron densities. *Nat. Commun.* **2019**, *10*, 4497.
(42) Le Roy, R. J.; Huang, Y.; Jary, C. An accurate analytic potential function for ground-state N 2 from a direct-potential-fit analysis of spectroscopic data. *J. Chem. Phys.* **2006**, *125*, 164310.
(43) Kaplan, A. D.; Levy, M.; Perdew, J. P. The predictive power of exact constraints and appropriate norms in density functional theory. *Annu. Rev. Phys. Chem.* **2023**, *74*, 193−218.
(44) Kowalski, K.; Piecuch, P. Renormalized CCSD (T) and CCSD (TQ) approaches: Dissociation of the N 2 triple bond. *J. Chem. Phys.* **2000**, *113*, 5644−5652.
(45) Larsson, H. R.; Zhai, H.; Umrigar, C. J.; Chan, G. K.-L. The chromium dimer: closing a chapter of quantum chemistry. *J. Am. Chem. Soc.* **2022**, *144*, 15932−15937.
(46) Zhang, Y.; Zhang, W.; Singh, D. J. Localization in the SCAN meta-generalized gradient approximation functional leading to broken symmetry ground states for graphene and benzene. *Phys. Chem. Chem. Phys.* **2020**, *22*, 19585−19591.
(47) Mejía-Rodríguez, D.; Trickey, S. Spin-crossover from a well-behaved, low-cost meta-GGA density functional. *J. Phys. Chem. A* **2020**, *124*, 9889−9894.
(48) Motta, M.; Ceperley, D. M.; Chan, G. K.-L.; Gomez, J. A.; Gull, E.; Guo, S.; Jiménez-Hoyos, C. A.; Lan, T. N.; Li, J.; Ma, F.; et al. Towards the solution of the many-electron problem in real materials: Equation of state of the hydrogen chain with state-of-the-art many-body methods. *Phys. Rev. X* **2017**, *7*, No. 031059.
(49) Grüning, M.; Gritsenko, O.; Van Gisbergen, S.; Baerends, E. The failure of generalized gradient approximations (GGAs) and meta-GGAs for the two-center three-electron bonds in He2+,(H2O) 2+, and (NH3) 2+. *J. Phys. Chem. A* **2001**, *105*, 9211−9218.
(50) Chayes, J.; Chayes, L.; Ruskai, M. B. Density functional approach to quantum lattice systems. *J. Stat. Phys.* **1985**, *38*, 497−518.
(51) Ullrich, C.; Kohn, W. Degeneracy in density functional theory: Topology in the v and n spaces. *Phys. Rev. Lett.* **2002**, *89*, 156401.
(52) Lammert, P. E. Coarse-grained V representability. *J. Chem. Phys.* **2006**, *125*, No. 074114.
(53) Mori-Sánchez, P.; Cohen, A. J.; Yang, W. Many-electron self-interaction error in approximate density functionals. *J. Chem. Phys.* **2006**, *125*, 201102.
(54) Pederson, M. R.; Ruzsinszky, A.; Perdew, J. P. Communication: Self-interaction correction with unitary invariance in density functional theory. *J. Chem. Phys.* **2014**, *140*, 121103.
(55) Schmidt, T.; Kümmel, S. One-and many-electron self-interaction error in local and global hybrid functionals. *Phys. Rev. B* **2016**, *93*, 165120.
(56) Yang, Z.; Pederson, M. R.; Perdew, J. P. Full self-consistency in the Fermi-orbital self-interaction correction. *Phys. Rev. A* **2017**, *95*, No. 052505.
(57) Savin, A.; Flad, H.-J. Density functionals for the Yukawa electron-electron interaction. *Int. J. Quantum Chem.* **1995**, *56*, 327−332.
(58) Iikura, H.; Tsuneda, T.; Yanai, T.; Hirao, K. A long-range correction scheme for generalized-gradient-approximation exchange functionals. *J. Chem. Phys.* **2001**, *115*, 3540−3544.
(59) Yanai, T.; Tew, D. P.; Handy, N. C. A new hybrid exchange−correlation functional using the Coulomb-attenuating method (CAM-B3LYP). *Chem. Phys. Lett.* **2004**, *393*, 51−57.
(60) Vydrov, O. A.; Scuseria, G. E. Assessment of a long-range corrected hybrid functional. *J. Chem. Phys.* **2006**, *125*, 234109.
(61) Chai, J.-D.; Head-Gordon, M. Long-range corrected hybrid density functionals with damped atom−atom dispersion corrections. *Phys. Chem. Chem. Phys.* **2008**, *10*, 6615−6620.
(62) Baer, R.; Livshits, E.; Salzner, U. Tuned range-separated hybrids in density functional theory. *Annu. Rev. Phys. Chem.* **2010**, *61*, 85−109.
(63) Grimme, S. Semiempirical hybrid density functional with perturbative second-order correlation. *J. Chem. Phys.* **2006**, *124*, No. 034108.
(64) Schwabe, T.; Grimme, S. Double-hybrid density functionals with long-range dispersion corrections: higher accuracy and extended applicability. *Phys. Chem. Chem. Phys.* **2007**, *9*, 3397−3406.
(65) Li, C.; Zheng, X.; Su, N. Q.; Yang, W. Localized orbital scaling correction for systematic elimination of delocalization error in density functional approximations. *Natl. Sci. Rev.* **2018**, *5*, 203−215.

https://doi.org/10.1021/acs.jpclett.3c03073
J. Phys. Chem. Lett. 2024, 15, 826−833

(66) Bao, J. L.; Wang, Y.; He, X.; Gagliardi, L.; Truhlar, D. G. Multiconfiguration pair-density functional theory is free from delocalization error. *J. Phys. Chem. Lett.* **2017**, *8*, 5616−5620.

(67) Su, N. Q.; Mahler, A.; Yang, W. Preserving symmetry and degeneracy in the localized orbital scaling correction approach. *J. Phys. Chem. Lett.* **2020**, *11*, 1528−1535.

(68) Georges, A.; Kotliar, G. Hubbard model in infinite dimensions. *Phys. Rev. B* **1992**, *45*, 6479.

(69) Kotliar, G.; Savrasov, S. Y.; Haule, K.; Oudovenko, V. S.; Parcollet, O.; Marianetti, C. Electronic structure calculations with dynamical mean-field theory. *Rev. Mod. Phys.* **2006**, *78*, 865.

(70) Andersson, Y.; Langreth, D. C.; Lundqvist, B. I. van der Waals Interactions in Density-Functional Theory. *Phys. Rev. Lett.* **1996**, *76*, 102−105.

(71) Vydrov, O. A.; Van Voorhis, T. Nonlocal van der Waals density functional: The simpler the better. *J. Chem. Phys.* **2010**, *133*, 244103.

(72) Parrish, R. M.; Burns, L. A.; Smith, D. G.; Simmonett, A. C.; DePrince, A. E., III; Hohenstein, E. G.; Bozkaya, U.; Sokolov, A. Y.; Di Remigio, R.; Richard, R. M.; et al. Psi4 1.1: An open-source electronic structure program emphasizing automation, advanced libraries, and interoperability. *J. Chem. Theory Comput.* **2017**, *13*, 3185−3197.

(73) Boerner, T. J.; Deems, S.; Furlani, T. R.; Knuth, S. L.; Towns, J. *Practice and Experience in Advanced Research Computing*; ACM, 2023; pp 173−176.

https://doi.org/10.1021/acs.jpclett.3c03073
J. Phys. Chem. Lett. 2024, 15, 826−833